SEMARAK ILMU PUBLISHING

Semarak Journal of Thermal-Fluid Engineering

Journal homepage:
https://semarakilmu.my/index.php/sjotfe/index
ISSN: 3030-6639

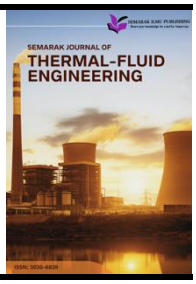

Analysis of Aerodynamics on Surface of the Car with Turbulence Models

Annur Adilia Maisarah Mat[1], Ishkrizat Taib[1,*], Muharis Mahbubi[1], Wan Nur Aina Afiqah Wan Jefri[1], Teor Wee Hock[1], Bukhari Mansoor[1], Normayati Nordin[1], Andril Arafat[2]

[1] Faculty of Mechanical and Manufacturing Engineering, Universiti Tun Hussein Onn Malaysia, 86400 Parit Raja, Batu Pahat, Johor, Malaysia
[2] Department of Mechanical Engineering, Faculty of Engineering, Universitas Negeri Padang, Indonesia

ARTICLE INFO

Article history:
Received 24 January 2025
Received in revised form 20 February 2025
Accepted 12 March 2025
Available online 27 March 2025

Keywords:
K-omega SST; k-epsilon; k-kl-omega; transition SST; ANSYS software; drag coefficient; lift; friction; turbulence models

ABSTRACT

The topology of the test vehicle was modeled using an Audi A4 and this study investigates the aerodynamic performance of an Audi car by analyzing the flow characteristics around its shape under different wind velocities and turbulence models. With a focus on improving fuel efficiency and reducing drag, the simulation aims to determine aerodynamics performance of a car through the analysis of drag and friction coefficients. The simulation involves detailed modelling of the car geometry, meshing and the application of the appropriate governing equations. The study also focuses on incompressible flow in the headwind direction and analyses the performance of one car geometry to meet these objectives. In this study, four cases were employed using CFD approach by setup model using k-epsilon, k-omega SST, Transition SST, and k-kl-omega on the flow behavior around the car. The results revealed that the k-omega SST model produced the lowest drag coefficient of 0.2547, indicating its effectiveness in reducing aerodynamic resistance. Conversely, the k-kl-omega model resulted in the highest lift coefficient of 0.0921, which could lead to increase aerodynamic lift. For friction coefficient analysis, k-omega SST exhibited the lowest value of 0.0026, making it the most reliable model for minimizing surface friction forces. Therefore, the k-omega SST model emerged as the most effective turbulence model, providing the optimal balance between drag, lift, and friction coefficients which making it ideal for optimizing the aerodynamic of the car performance. The analysis should be used to explore further improvements in vehicle design, including the surface modifications and vortex generators, to reduce drag force and to enhance the overall aerodynamic efficiency.

1. Introduction

The aerodynamic performance of vehicles plays a major role in improving fuel efficiency, reducing drag and enhancing the overall stability. In the recent past, Computational Fluid Dynamics (CFD) has emerged as a powerful tool for simulating and analysing the aerodynamic behaviour of car bodies under various flow conditions. Accurate simulations can provide valuable insights into the effects of design modifications on aerodynamic forces such as drag and lift, which are vital for performance

* *Corresponding author.*
E-mail address: iszat@uthm.edu.my

https://doi.org/10.37934/sjotfe.4.1.3551a

and efficiency of a car [1-3]. Without being affected by the advancement in CFD, challenges remain in achieving reliable and precise results due to factors such as turbulence modelling, quality of the mesh and the boundary condition set up [4]. Previous studies have discovered the aerodynamic analysis of vehicles with different focus on the influence of mesh quality and turbulence models [5-8]. These studies also have demonstrated that using finer meshes which generally leads to enhance accuracy, but at the cost of increased computational time and resources [9]. In vehicle aerodynamics studies, it is popular to use local mesh refinement near the surface of the vehicle and areas with high velocity gradients, while maintaining a coarser mesh in the far-field fluid domain for efficiency [10]. Reconstruction of the element grid for vehicle aerodynamics consumes more time as the flow of computational domain is relatively huge and not always be beneficial. By creating a well-distributed mesh from the beginning can eliminate the need for adaptive meshing [9].

Furthermore, turbulence models such as k-epsilon, k-omega SST, and transition SST have been widely used to predict the flow characteristics by offering different strengths and limitations depending on the complexity of the flow and the level of detailed required [11-15]. While these models are effective in many cases of study, comprehensive understanding of their performance under different conditions remains needed. Importance of accurate turbulence modelling in obtaining realistic flow simulations also have been highlighted in previous study which noting that the k-epsilon model is widely used, it often to underpredict certain flow phenomena such as flow separation especially in complex geometries [16-19].

However, there is a gap in the literature directly comparing the effects of different turbulence models and mesh resolutions on drag and lift force analysis in vehicle aerodynamics, especially at varying wind speeds as most previous studies have focused on either drag coefficient alone or specific turbulence models without a comprehensive comparison across models for real-world car geometries [20,21]. This study pursues to fill that gap by simulating the aerodynamic flow around an Audi A4 under headwind conditions by using four different turbulence models which are k-epsilon, k-omega SST, transition SST, and k-kl-omega which expect to contribute to a better understanding of how turbulence models and wind conditions affect the aerodynamic forces acting on the vehicle, which can inform future vehicle design improvements. This study also aims to assess the impact of wind velocity on the drag, friction and lift forces acting on the vehicle, providing a more nuanced understanding of how these factors interact in the real-world conditions. Additionally, there is a lack of studies that thoroughly examine the friction coefficient and its impact on vehicle stability under various scenarios which is crucial for high-speed applications.

Moreover, this research aims to address these gaps by investigating the flow characteristics around the Audi A4's aerodynamic shape for different wind velocities across various turbulence models. Furthermore, this study also emphasizes on the car's aerodynamic performance by analysing the drag and friction coefficients. The scope of the study is confined to the analysis of the drag coefficient and its forces under steady-state, incompressible flow conditions, with wind only in the headwind direction. The Computational Fluid Dynamics (CFD) method is employed for these simulations with the ANSYS Fluent software being used for meshing, simulation and analysis of the flow characteristics. Limitations include the use of a single vehicle geometry and the restriction of simulation to wind speeds withing the considered range.

2. Methodology

2.1 Geometry of an Audi Car A4 Model

This aerodynamic analysis of the Audi car model under various wind velocities includes the geometry of the car, discretization of meshing, governing equations, boundary condition parameters,

turbulence models used, and analysis of drag, lift coefficients and friction forces. In the simulation setup, the geometry used for external aerodynamic analysis consists of an Audi A4 2017 model which has dimensions of 1.43 m (H) x 4.73 m (L) x 1.84 m (W) (Figure 1). Meanwhile, the computational fluid domain is designed to encompass the car and allow for accurate analysis of airflow around it. The dimension of the fluid domain is bigger than the car which is 9 m (H) x 25 m (L) x 6 m (W). This domain size is to ensure that the car is sufficiently isolated from the boundaries to avoid any interference from the inlet and the outlet effect which provides adequate space for the airflow to develop before reaching the car and for capturing the wake phenomena behind it. The large domain also allows the software to capture the complex aerodynamic behavior including the turbulence and flow separation that occur during the simulation. The focus is on a single car geometry and the wind is applied in the headwind direction, 0˚.

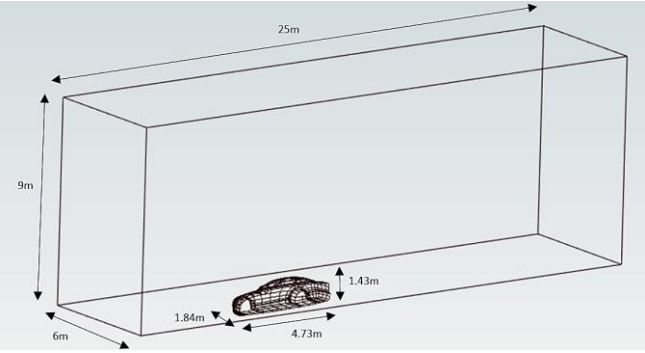

Fig. 1. Geometry of an Audi car A4 model

2.2 Discretization of Meshing

To ensure precision and reliability of the simulation results, mesh refinement was applied to the geometry. The computational domain was discretized by using an unstructured mesh of varying element sizes, and a Grid Independence Test (GIT) validated that the mesh size does not significantly affect the drag coefficient and the aerodynamic forces. In addition, three mesh densities were tested, focusing on refining the critical areas such as the surface of the car, including the front, rear and underbody regions where the velocity and pressure gradients were completely high. Inflation layers with 5 layers and a growth rate of 1.2 were added near the surface of the car to capture the boundary layer flow near the surface of the car by ensuring the accurate computation of wall effects and friction. The final mesh used in the simulation consisted of 416,080 elements with high quality elements near the boundary layer, ensuring the mesh independent and accurate aerodynamic analysis. Figure 2 shows the mesh densities around the car body.

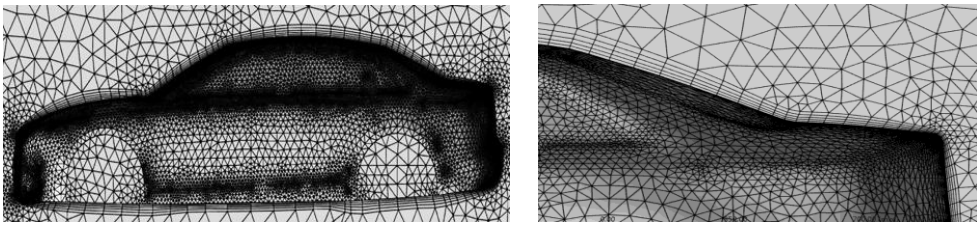

(a) (b)

Fig. 2. Mesh refinement around the surface of car (a) Full body of car (b) Inflation layer at car surface

2.3 Governing Equations

The simulation of the airflow around the car is modeled as a steady-state and turbulent flow. The fluid is inviscid and incompressible while the mean density and pressure are uniform throughout the fluid. This study is based on Reynolds-Average Navier-Stokes (RANS) equations, along with different turbulence models used which is solved by using finite volume method. The governing equations for the simulation are the continuity and momentum equations, which are expressed as follows. Continuity equation used to ensure the conservation of mass in the incompressible flow.

$$\frac{\partial \boldsymbol{u}}{\partial \boldsymbol{x}} + \frac{\partial \boldsymbol{v}}{\partial \boldsymbol{y}} + \frac{\partial \boldsymbol{w}}{\partial \boldsymbol{z}} = \mathbf{0} \tag{1}$$

where $\frac{\partial \boldsymbol{u}}{\partial \boldsymbol{x}}$ is rate of change of velocity component u in x-direction, $\frac{\partial \boldsymbol{v}}{\partial \boldsymbol{y}}$ is rate of change of velocity component v in y-direction and $\frac{\partial \boldsymbol{w}}{\partial \boldsymbol{z}}$ is rate of change of velocity component w in z-direction.

$$\nabla \cdot v = 0 \tag{2}$$

where $\boldsymbol{v}$ is the velocity vector of u, v and w of the fluid. While ∇ is the representing spatial derivatives. Momentum equation for inviscid and incompressible flow:

$$\rho\left(\frac{\partial v}{\partial t} + v \cdot \nabla v\right) = -\nabla \mathrm{P} + \mathrm{F} \tag{3}$$

$$\rho v \cdot \nabla v = -\nabla \mathrm{P} \tag{4}$$

where ρ is density of the fluid (kg/m^3), v is the velocity vector of fluid, P is the pressure (Pa), F are external body forces per unit volume and ∇P is pressure gradient.

The aerodynamic performance of the car is quantified through the drag and friction coefficients at different wind velocities which are calculated using these formulas respectively:

$$C_d = \frac{F_d}{\frac{1}{2}\rho V^2 A} \tag{5}$$

where ρ is density of the fluid (kg/m^3), F_d is the drag force, V is the wind velocity (m/s), A is the reference area and C_d is drag coefficient.

$$C_l = \frac{F_l}{\frac{1}{2}\rho V^2 A} \tag{6}$$

where F_l is the lift force, and C_l is lift coefficient.

$$C_f = \frac{\tau_\omega}{\frac{1}{2}\rho V^2} \tag{7}$$

where τ_ω is wall shear stress (Pa) and V is the wind velocity (m/s).

The drag, friction and lift coefficient are analysed for various wind speeds and compared across four different of turbulence models. These values are crucial in fluid dynamics which shaping the

design and operation of countless technologies. While drag resist motion, friction coefficient in car simulation is crucial for understanding the impact of surface resistance on the overall aerodynamic performance. Friction influences drag, as higher friction leads to greater resistance, reducing fuel efficiency and performance while lower friction helps to minimize the drag. By analysing friction, car surface design for smoother airflow can be optimized, improving aerodynamic efficiency, reduce energy loss and enhance overall performance of the car.

2.4 Boundary Condition Parameters

As for the boundary conditions (Figure 3), the simulation is set up with a velocity inlet where wind velocities vary from low to high, representing different wind speed based on real world scenarios. With a constant headwind, the airflow hits the car directly at angle of (0˚), typically causing the highest drag. These velocity choices influence drag, lift, friction and flow separation which is crucial for fuel efficiency, stability and control. The velocity parameter reflects the real-world scenarios. A pressure outlet at the back of the computational domain is maintained at atmospheric pressure. Furthermore, the surface body of the car is modeled with a no-slip condition to accurately capture the friction forces acting on the body. The ground of the domain is treated as a moving wall which matches the velocity of the inlet to simulate the motion of the car relative to the ground. In this simulation, this boundary remained stationary. Moreover, symmetry boundary conditions are applied to reduce the computational cost by limiting the flow domain. In addition, four different types of turbulence models such as k-epsilon, k-omega SST, transition SST and k-kl-omega are used to evaluate different turbulent flow around the Audi car model.

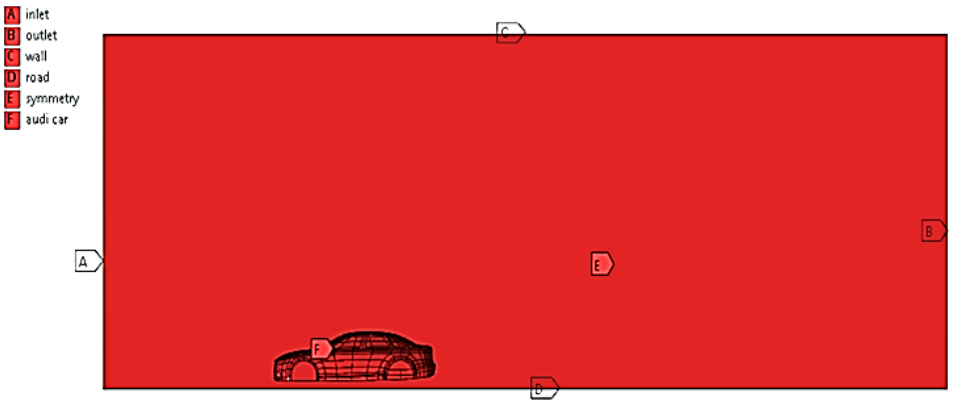

Fig. 3. Boundary conditions of an Audi car geometry

2.5 Grid Independence Test (GIT)

Grid Independence Test (GIT) is an important technique for validating the results which verifies the whole simulation outcomes are not dependent on mesh resolution [22]. It is vital for ensuring the accuracy and reliability of Computational Fluid Dynamics (CFD) simulations, particularly in the aerodynamic analysis of the Audi Car. Moreover, GIT is important in verifying the numerical accuracy of CFD model, especially in complex flow simulation [23]. By refining the mesh resolution, the test helps determine when the simulation results such as drag, friction and lift coefficients become independent of the grid size. This also ensures that the results are not significantly influenced by the mesh resolution, but it does reflect the actual behavior around the car. GIT also plays an important role in optimizing computational resources, as finer meshes increase the computational time and memory requirements. By performing the test, it helps to avoid numerical errors or inaccuracies in

the simulation results that may arise from an inadequate mesh and increase the confidence in the validity of the simulation results.

2.6 Quantification of Drag, Lift, and Friction Coefficient

The analysis in this study focuses on quantifying the drag, lift, and friction coefficients to evaluate the aerodynamic performance of the car under various conditions. These coefficients are critical in determining the resistance of the vehicle faces as it moves through the air, with the drag coefficient influencing aerodynamic resistance, the lift coefficient affecting the stability of the vehicle, and the friction coefficient related to the surface interactions. The model is tested under different wind velocities, ranging from low to high-speed condition range from 3 m/s to 60 m/s, is to observe its aerodynamic behavior across various real-world scenarios. As velocity increases, the drag force generally rises due to its quadratic relationship with speed, while the lift coefficient behavior is more complex and depends on the shape of the car and its flow characteristics.

Four turbulence models were employed to study for the effects of turbulent flow which include k-epsilon, k-omega SST, transition SST, and k-kl-omega. These models allow the study of different flow regimes and their impact on the aerodynamic of the car, with each model providing unique insights into flow separation, boundary layers and pressure distribution. By using multiple turbulence models and wind velocities, this study is to ensure a comprehensive evaluation of the performance of the car, which contributes to a better understanding of the most suitable model for predicting aerodynamic forces and improve the design of the vehicle.

3. Results and Discussions

Aerodynamic performance of the Audi Car model is analysed for different wind velocities across turbulence models which is presented include drag friction and lift coefficients as well as the corresponding forces acting on the vehicle. Flow characteristics such as flow separation and vortex formation are discussed based on the turbulence models used in the simulations.

3.1 Velocity Distribution

3.1.1 K-omega SST model

The velocity distribution across the k-omega SST model in Figure 4. For various wind velocities demonstrate clear insights into the aerodynamic behavior and flow separation around the surface of the car. Based on the velocity distribution in Figure 4(a) to Figure 4(f) across K-omega SST model, it shows a clear progression of flow behavior as wind velocity increases. Flow remains largely attached to the surface of the car at the lowers speed in (a), with minimal turbulence and a small wake. As velocity increases, flow separation begins, particularly near the roof and rear which leads to a more turbulent wake region. At medium to high speed such in (d), (e), (f), the wake becomes significantly larger, with pronounced turbulence and flow detachment, particularly at the rear. The k-omega SST model captures this transition from laminar to turbulent flow effectively, highlighting its ability to predict flow separation and wake formation, especially at high velocities.

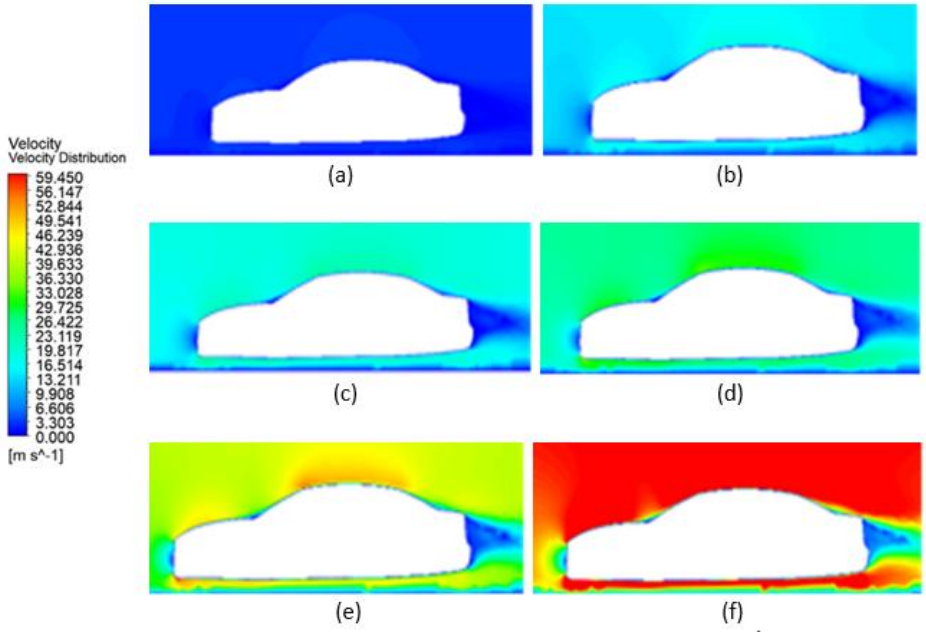

Fig. 4. Velocity distribution across K-omega SST model (a) Light breeze (3 m/s) (b) Coastal highway (14 m/s) (c) Stormy weather (18 m/s) (d) Severe weather (25 m/s) (e) Hurricane-force wind (40 m/s) (f) Tornado-level wind (60 m/s)

3.1.2 Transition SST model

The velocity distribution across the Transition SST model shows a distinct transition from laminar to turbulent flow as wind velocity increases. In the Figure 5(a), flow remains mostly attached to the surface of car, with a smooth distribution and smaller wake region behind the car. As the velocity increases, a transition to turbulence occurs, with flow separation beginning near the rear of the car in which resulting in a larger wake.

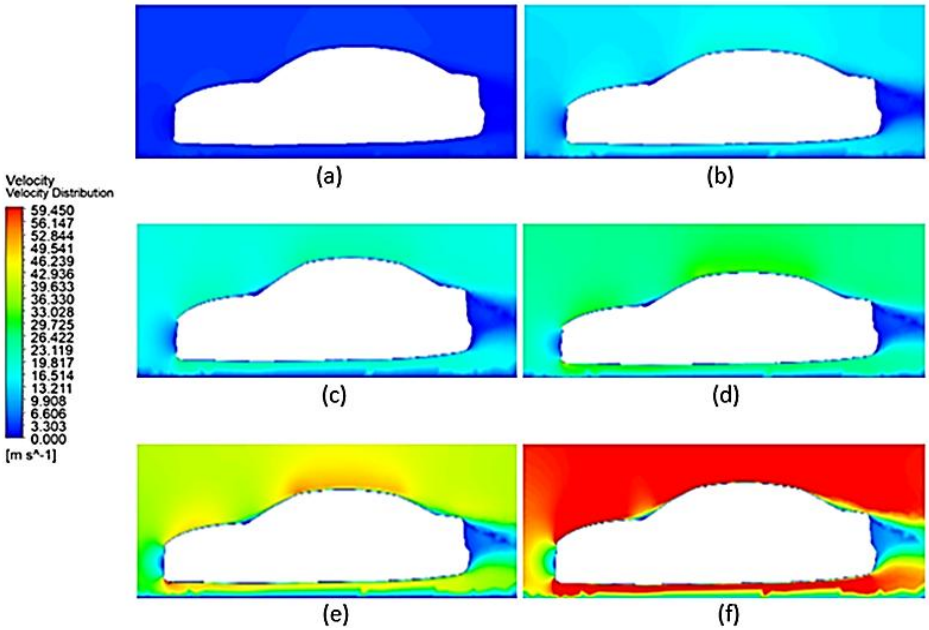

Fig. 5. Velocity distribution across transition SST model (a) Light breeze (3 m/s) (b) Coastal highway (14 m/s) (c) Stormy weather (18 m/s) (d) Severe weather (25 m/s) (e) Hurricane-force wind (40 m/s) (f) Tornado-level wind (60 m/s)

Subsequently, turbulence become more pronounced, and a significant wake region develops indicates higher level of drag at high velocities. This model is effectively in capturing early flow transitions from laminar to turbulent, especially around the edges of the car, making it valuable for cases where flow transition needs to be predicted accurately at moderate velocities.

3.1.3 K-kl omega model

The velocity distribution across k-kl-omega model such in Figure 6 demonstrates a distinct transition from laminar to turbulent flow across various wind velocities. Based on Figure 6, The flow remains mostly attached to the surface of the car at the lower speed in (a) with limited signs of separation, indicating a laminar-dominated regime. The model effectively captures the early onset of turbulence, with flow separation occurring more gradually compared to other models when the wind speeds increases. Notably, at high velocities such in (d), (e), and (f), the wake region is broader but the transition between attached and separated flow is smoother which reflecting the focus of the model is on predicting transitional behaviours. The k-kl-omega model provides a better representation of transitional flows in which is evident in its ability to capture mixed laminar-turbulent regime and gradually separation at medium speeds.

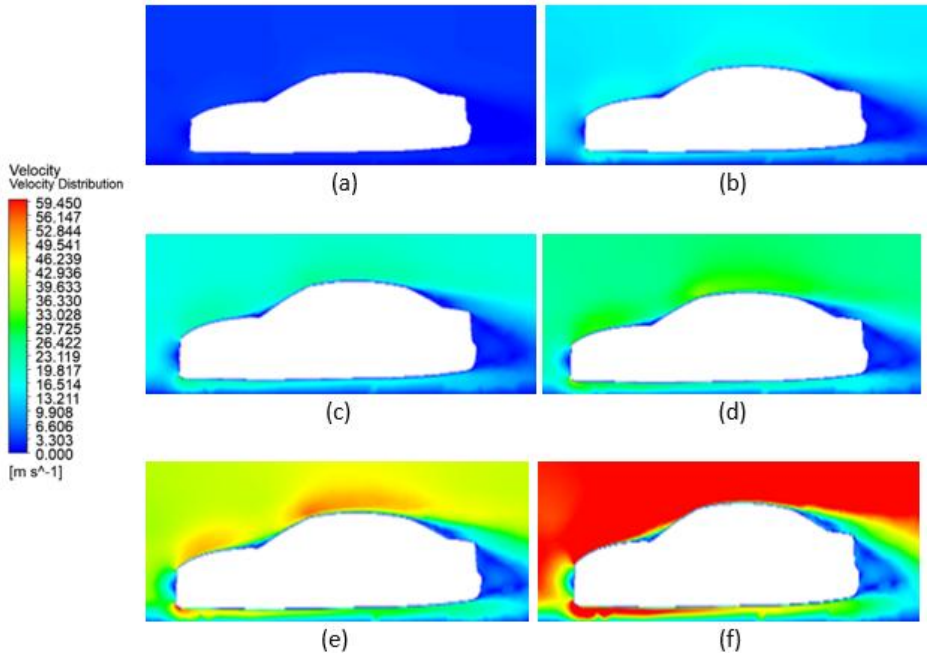

Fig. 6. Velocity distribution across l-kl-omega model (a) Light breeze (3 m/s) (b) Coastal highway (14 m/s) (c) Stormy weather (18 m/s) (d) Severe weather (25 m/s) (e) Hurricane-force wind (40 m/s) (f) Tornado-level wind (60 m/s)

3.1.4 K-epsilon model

The velocity distribution across the k-epsilon model such in Figure 7. has revealed characteristics typical of fully turbulent flow predictions. Based on Figure 7, the flow tends to separate more abruptly from the car body, especially at the rear as the speed increases. The wake regions behind the car grow significantly in size as velocity increases, with the largest wake observed at the highest wind speed such as Figure 7(f). The tendency of this model is to predict more pronounced separation zones, even at moderate speeds shows that it may be over-predicting the turbulence intensity in comparison to model such k-omega SST or k-kl-omega. The k-epsilon model generally performs well

in fully developed turbulent flows but is less accurate for predicting transitional flow regimes which explains the larger and less controlled wake areas seen at higher speeds. Consequently, while it provides reasonable results at high Reynolds numbers, it lacks the precision needed for more nuanced transition between laminar and turbulent flow, leading to more abrupt flow separation and less favorable aerodynamics.

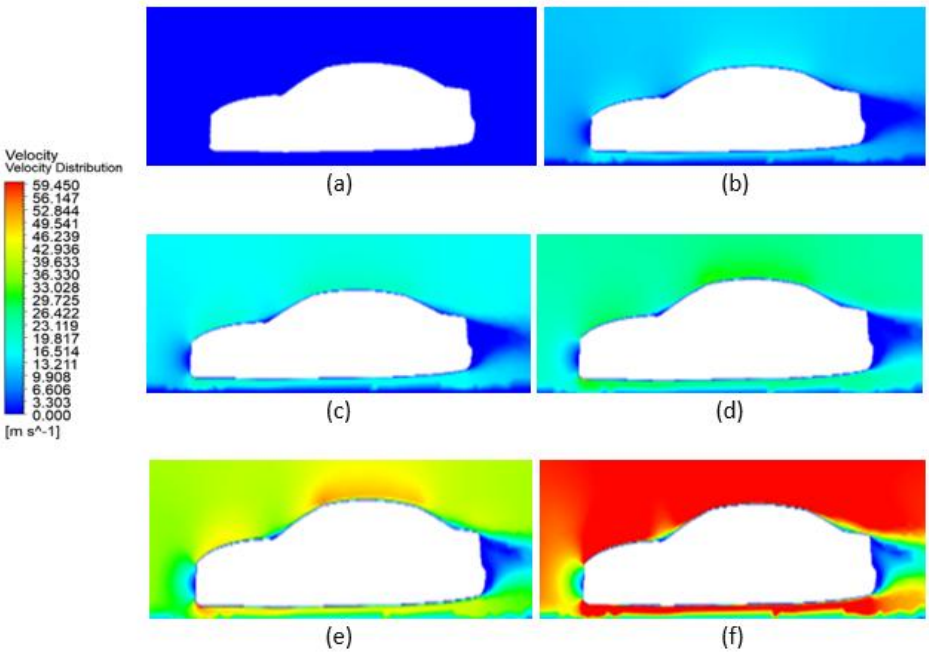

Fig. 7. Velocity distribution across k-epsilon model (a) Light breeze (3 m/s) (b) Coastal highway (14 m/s) (c) Stormy weather (18 m/s) (d) Severe weather (25 m/s) (e) Hurricane-force wind (40 m/s) (f) Tornado-level wind (60 m/s)

3.2 Pressure Distribution

To effectively analyze the aerodynamic characteristics of the car under different wind conditions, a detailed examination of the pressure distribution is vital. Among other wind speeds considered in this study, the high-speed condition (60 m/s) provides the most comprehensive insights into the wake regions and flow separation around the car. The flow exhibits more pronounced separation and turbulent wake formation, which significantly impacts the aerodynamics of the car. Therefore, pressure distribution contour for 60 m/s wind speed has been selected for visualization as it reveals the critical details about the pressure variation along the car body, especially in regions where flow separation occurs which is essential for understanding the overall aerodynamic performance.

Based on Figure 8, the pressure distribution on the car surface reveals key aerodynamic interactions. The top view of the car in Figure 8(c) shows high pressure at the front due to air stagnation, with pressure decreasing as airflow accelerates over the roof which indicate effective streamlining but potential wake formation at the rear. The front view such in Figure 8(a) highlights a central high-pressure zone caused by air impact while rear view reveals low pressure region due to flow separation which led to vortex formation and aerodynamic drag. From the side view in Figure 8(b), pressure decreases along the surface of the car as air moves from the front to the rear indicating boundary layer development and reattachment points. These patterns emphasize the importance of reducing frontal stagnation pressure and optimizing the rear design, such as tapering or adding diffusers which to minimize the wake size, reduce drag, and improve aerodynamic efficiency. Table 1 shows the average pressure drop from various wind speeds across difference turbulence models.

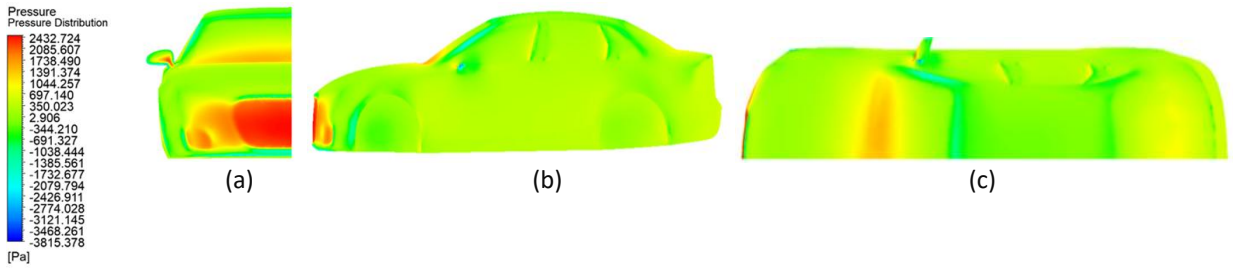

Fig. 8. Pressure distribution on surface of car at 60 m/s (a) Front view (b) Side view (c) Top view

Table 1
Average pressure on car body in different velocity across turbulence models

Velocity of wind (m/s)	Average pressure on surface of Audi car (Pa)			
	K omega SST	Transition SST	k-kl-omega	k-epsilon
3	-1.142	-1.146	-0.406	-2.320
14	-25.920	-26.072	-0.305	-27.311
18	-43.164	-43.347	-6.688	-42.480
25	-84.454	-84.319	-25.381	-82.620
40	-216.879	-218.391	-103.306	-213.762
60	-491.086	-494.526	-312.813	-484.415

Table 1 and graph shown in Figure 9 provide data on the average pressure drop at the surface of the car across different wind speeds for four turbulence models: k-Omega SST, Transition SST, k-kl Omega, and k-Epsilon. Based on Figure 9, the graph illustrates that both k-omega SST and transition SST model predict consistent and realistic pressure drops with increasing wind speed in which indicating their reliability for capturing near-wall turbulence, flow separation, and reattachment. The k-kl-omega model underpredicts pressure drops, reflecting its limitation in handling boundary layer interactions and wake effects. Conversely, the k-epsilon model overpredicts pressure drop due to its inability to accurately capture near-wall flow phenomena which result in exaggerating wake turbulence. The k-omega SST model stands out as the most reliable for this simulation, with predictions that align well with theoretical expectations and the observed pressure distributions contour. These findings reinforce the suitability of k-omega SST for high-speed aerodynamic simulations, as it accurately captures pressure gradients and flow dynamics critically to evaluating the aerodynamic performance of the car.

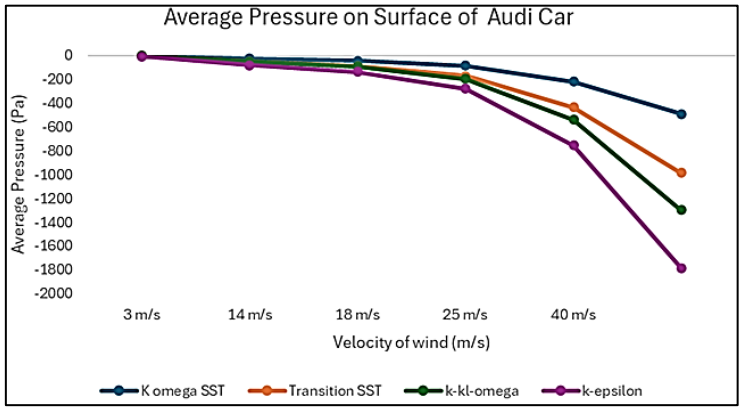

Fig. 9. Average pressure on surface of car

3.3 Drag Coefficient (C_d) and Drag Force (N)

The results highlight the impact of different turbulence models on drag predictions. Table 2 presents the drag coefficients, and its forces act on the surface of the car body in different velocity across various turbulence models. Based on the graphs plotted in Figures 10(a) and 10(b), the analysis of drag coefficients and drag force has revealed key differences between turbulence models across various wind velocities. The drag coefficient increases as the velocity of wind rises for all model types which is expected due to the quadratic relationship between drag and velocity. The differences between turbulent models become more significant at higher velocities, suggesting that turbulence modelling become increasingly important as the flow becomes more turbulent. Among them, k-kl-omega consistently predicts the highest drag coefficients which indicating a stronger response to turbulence and flow separation, especially at higher speeds. Conversely, k-epsilon model predicts the lowest drag coefficient, reflecting a less sensitive approach to turbulent flow. The k-omega SST and transition SST models exhibit similar behaviour with moderate coefficients increases, aligning closely in their predictions. Moreover, both models are typically used for flows with adverse pressure gradients and separation.

Table 2
Drag coefficients and forces in different velocity across turbulence models

Wind speed category	Velocity (m/s)	K-omega SST		Transition SST		K-kl Omega		K-epsilon	
		Cd	Drag force, N	Cd	Drag force, N	Cd	Drag force, N	Cd	Drag force, N
Low	3	0.2547	1.4039	0.3506	1.9328	0.3506	1.9328	0.8915	4.9146
	14	5.1982	28.6550	0.3491	41.9101	0.3491	41.9101	0.2758	33.1112
Medium	18	8.5067	46.8930	8.5067	46.8930	0.3535	70.1522	0.2414	47.9007
	25	16.5672	91.3269	16.5672	91.3269	0.3594	137.5946	0.2404	92.0176
High	40	41.6718	229.7159	41.6718	229.7159	0.3652	357.8982	0.2393	234.4778
	60	93.6261	516.1140	93.6261	516.1140	0.3702	816.2123	0.2382	525.2014

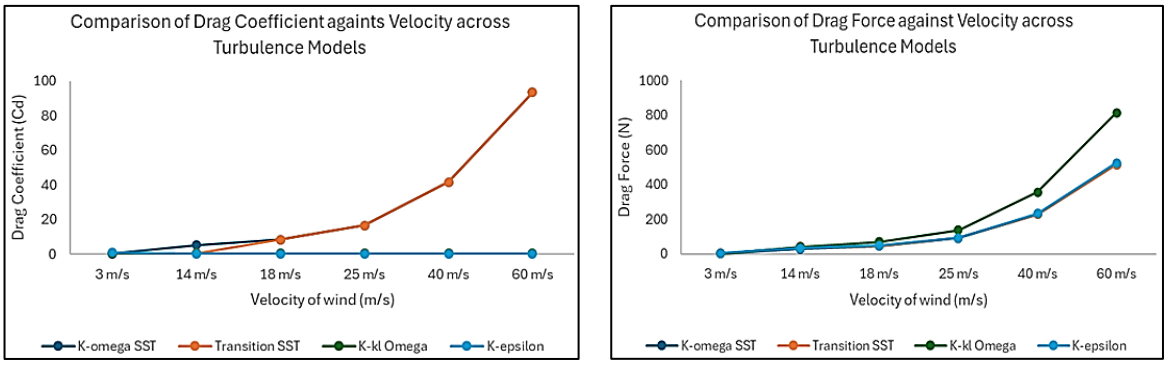

(a) (b)

Fig. 10. Comparison of drag against velocity across turbulence models (a) Drag coefficients (b) Drag force (N)

On the other hand, K-kl-omega is known for its transition capabilities and might be overpredicting drag due to its sensitivity to transition zones in the flow. While k-epsilon is computationally efficient, it might be underpredicting drag because it tends to perform better in free shear flows rather than boundary layer-driven flows. Moreover, regarding the drag force act on the surface body of the car, there is a significant rise as wind velocity increases, showing a quadratic relationship between velocity and drag. K-kl-omega again predicts the highest drag force which highlighting more substantial turbulence and aerodynamic resistance. In contrast, k-epsilon model predicts the lowest

drag force at higher velocities. The K-omega SST and transition SST models offer balanced drag force predictions which making them suitable for general aerodynamic analysis with moderate turbulence effect. Overall, based on the data presented above, k-kl-omega proves highly sensitive to velocity changes, while k-epsilon provides a more conservative approach, and the other two models offer a middle ground for analysing drag and turbulence.

3.4 Lift Coefficient (C_l) and Lift Force (N)

Table 3 and graphs in Figures 11(a) and 11(b) present the lift coefficients and lift forces for different wind velocities across various turbulence models. The results reveal several trends and their potential impact on the aerodynamic performance of the car. The analysis of lift coefficients and forces across different wind velocities shows that most turbulence models predict negative downforce which improves the stability of the car and handling by increasing the grip of tires especially at medium and high speeds. Both k-epsilon and k-omega SST models consistently show significant downforce, with increasing negative forces as the velocity of the wind rises while enhancing the aerodynamic performance. Moreover, this also suggests that different turbulence models predict varying degrees of lift forces at lower speeds which could impact the stability of the car but not significantly since the forces are low. The negative downforce helps to press the car to the ground by increasing the tires grip and minimizing the risk of the vehicle losing control due to lift.

However, the lift behavior varies across different turbulence models which suggest that model selection can significantly influence predictions of aerodynamics. It can be seen in the k-kl-omega model which exhibits positive lift coefficient and forces at high speed (40 m/s and 60 m/s) that indicates that it predicts some lift instead of downforce. The positive lift could reduce the stability of the car by reducing downforce and making the vehicle more prone to lift at higher velocities. The positive value of k-kl-omega could be due to its focus on transition prediction, as it models the transition from laminar to turbulent flow more accurately. This might cause it to capture the areas of localized lift that other models treat as fully turbulent, leading to a different force prediction. Since the study focuses on lift forces in high-speed turbulent flow, k-omega SST model might be more suitable because they tend to predict the overall turbulent behavior and downforce more consistently.

Table 3
Lift coefficients and forces in different velocity across turbulence models

Wind speed category	Velocity of wind (m/s)	K-omega SST		Transition SST		K-kl omega		K-epsilon	
		Cl	Lift force, N	Cl	Lift force, N	Cl	Lift force, N	Cl	Lift force, N
Low	3	-0.1206	-0.6650	0.0049	0.0269	0.0049	0.0269	-3.5549	-19.5964
	14	-2.6602	-14.6646	0.0246	2.9520	0.0246	2.9520	-0.4853	-58.2637
Medium	18	-4.2377	-23.3605	-4.2377	-23.3605	0.0362	7.1799	-0.1528	-30.3224
	25	-7.7110	-42.5071	-7.7110	-42.5071	0.0474	18.1496	-0.1525	-58.3836
High	40	-20.296	-111.884	-20.2965	-111.8847	0.0709	69.5035	-0.1550	-151.9078
	60	-43.454	-239.542	-43.4544	-239.5424	0.0921	203.1536	-0.1562	-344.5194

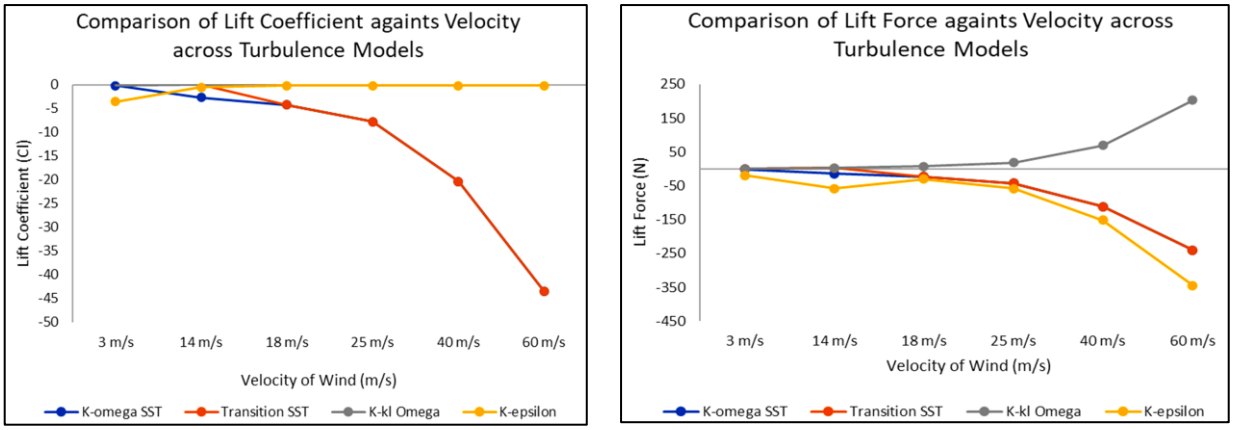

(a) (b)

Fig. 11. Comparison of lift against velocity across turbulence models (a) Lift coefficients (b) Lift force (N)

3.5 Skin Friction Coefficient (C_f)

Skin friction coefficient measures the frictional force per unit area acting on the surface of the car due to the boundary layer of air. It has derived from the wall to shear stress on the surface. Table 4 shows the friction coefficient of the simulation. Based on the Table 4 and graph presented in Figure 12(a) above, friction coefficient generally decreases as velocity of the wind increases across all turbulence models. This behavior is expected because higher velocities typically lead to thinner boundary layers which result in lower frictional forces. From the graph also we can conclude that the models of K-omega SST and transition SST show similar trends which suggest that these models predict smoother flow behavior and lower friction at higher speeds. Conversely, coefficient friction or friction drag in k-kl-omega model remains relatively high even at higher velocities which indicates that this turbulence model predicts more intense turbulent flow and higher resistance on the car surface.

In addition, results in k-epsilon models slightly higher than those of k-omega SST and transition SST but lower than k-kl-omega which shows a smooth decrease in friction with increasing velocity, suggesting a moderate level of turbulence and resistance. The graph in Figure 12 visually supports the analysis of the impact of different turbulence models on the aerodynamic performance of the car as it highlights how lower skin friction as seen in k-omega SST and transition SST contributes to lower drag and better overall performance, while the higher skin friction in k-kl-omega indicates less efficient aerodynamic behavior.

Table 4
Friction coefficients and forces in different velocities across turbulence models

Velocity of wind (m/s)	Skin friction coefficient Cf			
	K omega SST	Transition SST	k-kl-omega	k-epsilon
3	0.00453	0.00453	0.00748	0.00461
14	0.00338	0.00336	0.00713	0.00358
18	0.00324	0.00321	0.00727	0.00344
25	0.00306	0.00303	0.00750	0.00329
40	0.00282	0.00280	0.00790	0.00307
60	0.00264	0.00262	0.00837	0.00290

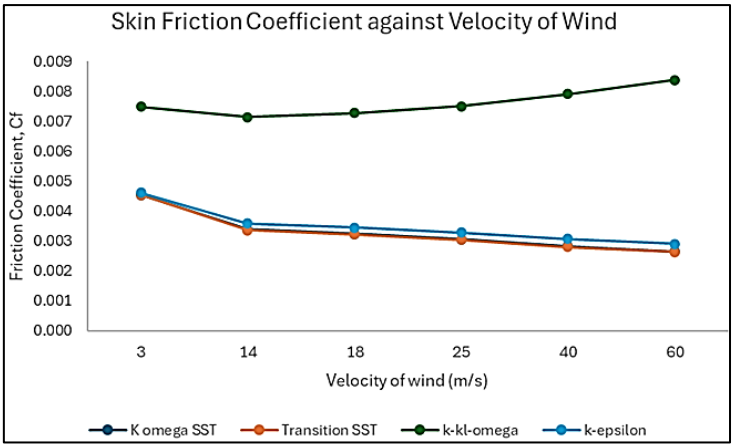

Fig. 12. Friction coefficient against velocity across turbulence models

Since the drag coefficient shown in Figure 10 increases with velocity while the friction coefficient in Figure 12 decreases, it suggests that the flow behavior around the car is changing with the increase in wind speed and it has implications for the performance of aerodynamic of the car. The increase in drag coefficient with velocity suggests that the shape of the car might not be ideal for high-speed flow, particularly minimizing the pressure drag. The decrease in friction indicates that the car is experiencing more turbulent flow, which reduces skin friction but increases overall drag. To optimize the aerodynamic performance, flow separation and turbulence in wake need to be reduced especially at higher speeds.

3.6 Grid Independence Test (GIT)

Three different mesh refinement levels were used in GIT, and the corresponding pressure and velocity profiles along a defined path were compared. As shown in the pressure and velocity in Table 5, the results from different meshes have converged closely to one another, with only minor variations between the finest and coarsest meshes. The pressure distribution along the path shows a characteristic of the pressure drop followed by recovery, which is consistent across all the mesh levels. Correspondingly, the velocity profile displays an increase in velocity in specific regions of the flow, followed by stabilization. The convergence of these results indicate that the mesh is fine enough to capture the flow physics accurately and further refinement would not significantly affect the results. Table 5 below shows the mesh level corresponding to the number of elements obtained with the pressure drop and maximum velocity.

Table 5
Comparison between mesh Levels

Mesh level	Element size (mm)	No. of elements	Pressure drop (Pa)	Maximum velocity (m/s)
Coarse	1500	415860	3.9222	25.00085
Medium	1500	515999	4.0645	25.99980
Fine	1500	416080	3.7928	25.00039

The percentage difference between mesh levels can be calculated by using the data of the pressure drop and the maximum velocity across the mesh level. From the table we can conclude that the number of elements increases while the mesh level getting finer. The percentage difference in velocity and pressure between the mesh level is calculated by using the formula below:

$$\% \text{ difference } = \frac{|V_{fine} - V_{medium}|}{V_{medium}} \times 100\% \quad (7)$$

$$\% \text{ difference } = \frac{|25.00039 - 25.99980|}{25.99980} \times 100 = 3.884\% \quad (8)$$

This has been proven that the solution is converged, and the mesh is sufficient to this simulation since the percentage different is only 3.884%, showing the percentage difference is small enough. The number of elements also indicates the highest at the fine level. Generally, the percentage difference below 5% is considered as acceptable level of variation in most engineering simulations. Since the calculated value is less than 5%, it validates the solution can be deemed grid-independent and further refining mesh is unlikely to result in significant changes to key simulation outcomes such as pressure, velocity and drag coefficient.

Based on the Figure 13(a) which is specifically show on how pressure varies along path in the simulation domain. The three lines correspond to different levels of mesh refinement. Ideally, as the mesh is refined, the results from the mesh levels should be converged which would suggest that the solution is grid independent. In Figure 13 shows all the three lines are observed that as the mesh get finer, the pressure curves are very close to each other with only minor differences. This indicates that the mesh is fine enough and that further refinement would not significantly change the pressure results. In addition, the general shape of the curve shows a drop in pressure, followed by recovery as move along the x-axis which is typical flow around a body where it expects pressure drop in a separation region or due to wake formation. The convergence of the different mesh results suggests that the solution is reliable.

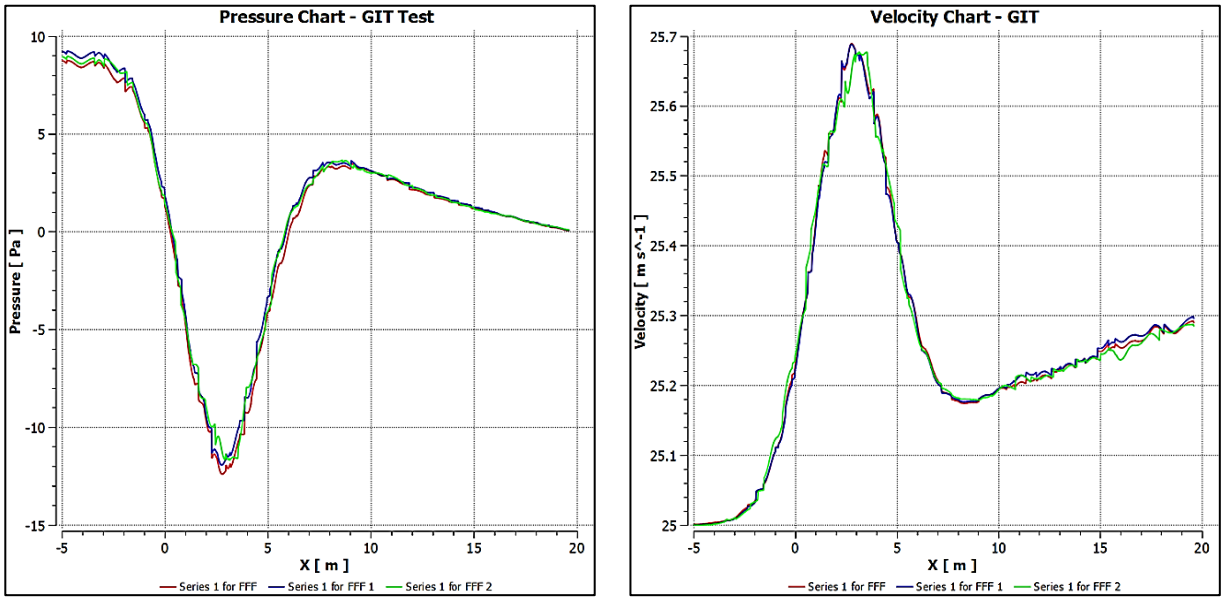

(a) (b)

Fig. 13. (a) Pressure chart for grid independence test (b) Velocity chart for GIT

Furthermore, the velocity chart in Figure 13(b) also shows a similar trend where the velocity varies along the x-axis. There is a peak in velocity, followed by a drop and the stabilization which could correspond to the acceleration of the floe in certain regions such as over the top of the car or around the sharp corner such inside mirror, and it decelerates as the flow separates or reattached. Like in pressure chart, the velocity profiles for different mesh refinements are very comparable which

again suggests grid independence. Therefore, the solution can be considered as grid-independent, and the chosen mesh is adequate for further analysis.

4. Conclusions and Recommendation

Based on the simulation and findings conducted in this study, the objectives of this study which includes investigating the aerodynamic performance of an Audi car under different wind velocities and turbulence models have been met. The analysis of drag and lift coefficients has revealed that drag increased with velocity, showing the rise in aerodynamic resistance at higher speeds, while the lift coefficient varied depending on the turbulence model used. Among the turbulence models, K-omega-SST provided the most reliable results for predicting both drag and lift forces, though k-kl-omega and transition SST demonstrated potential in capturing specific flow behaviors. The velocity distribution analysis showed increased turbulent flow and wake formation at higher speeds which affected the overall dynamic performance. Furthermore, it was also observed that the friction coefficient decreased as velocity of the wind increased, reflecting its reduced impact at higher speeds where pressure drag became more dominant. However, the overall aerodynamic performance can be further enhanced by refining the geometry of the car, particularly in the area that is prone to flow separation.

Future recommendations include optimizing the rear design of the car to minimize the drag, smoothing surfaces to manage turbulent airflow, and improving the underbody design to reduce turbulence. Moreover, exploring more advanced turbulence models such as Large Eddy Simulations (LES) or Detached Eddy Simulations (DES) could provide greater accuracy in predicting turbulent flow behavior. In summary, this study has provided valuable insights into the aerodynamic behavior of the car, with a focus on drag and lift forces. The objectives were successfully achieved, and the findings offer a solid foundation for future research and design improvements to enhance the overall aerodynamics performance of the car.

Acknowledgement

This research was supported by the Ministry of Higher Education of Malaysia through the Fundamental Research Garat Scheme (FRGS/1/2024/TK10/UTHM/02/6) and through MDR grant (Q686).

References

[1] Hucho, Wolf-Heinrich, ed. *Aerodynamics of road vehicles: from fluid mechanics to vehicle engineering*. Elsevier, 2013.

[2] Molla, Kibret. "A study of aerodynamic pressure drag and skin friction resistance comparison on ICE 3 train under different yaw-angles: Aerodynamic pressure drag and skin friction resistance." *Ethiopian Journal of Engineering and Technology* 3, no. 1 (2023): 1-24.

[3] Kamal, Muhammad Nabil Farhan, Izuan Amin Ishak, Nofrizalidris Darlis, Daniel Syafiq Baharol Maji, Safra Liyana Sukiman, Razlin Abd Rashid, and Muhamad Asri Azizul. "A review of aerodynamics influence on various car model geometry through CFD techniques." *Journal of Advanced Research in Fluid Mechanics and Thermal Sciences* 88, no. 1 (2021): 109-125. https://doi.org/10.37934/arfmts.88.1.109125

[4] Wang, J., D. Liu, G. Gao, Y. Zhang, and J. Zhang. "Numerical investigation of the effects of sand collision on the aerodynamic behaviour of a high-speed train subjected to yaw angles." *Journal of Applied Fluid Mechanics* 12, no. 2 (2019): 379-389. https://doi.org/10.29252/jafm.12.02.28788

[5] Murad, Nurul M., Jamal Naser, Firoz Alam, and Simon Watkins. *Simulation of vehicle A-pillar aerodynamics using various turbulence models*. No. 2004-01-0231. SAE Technical paper, 2004. https://doi.org/10.4271/2004-01-0231.

[6] Ansari, Abdul Razzaque. "CFD analysis of aerodynamic design of tata Indica Car." *International Journal of Mechanical Engineering and Technology* 8, no. 3 (2017): 344-355.

[7] Damjanović, Darko, Dražan Kozak, Marija Živić, Željko Ivandić, and Tomislav Baškarić. "CFD analysis of concept car in order to improve aerodynamics." *Járműipari innováció* 1, no. 2 (2011): 108-115.
[8] Buscariolo, Filipe Fabian, Felipe Magazoni, Marc Wolf, Flavio Koiti Maruyama, Julio Cesar Lelis Alves, and Leonardo José Della Volpe. *Analysis of turbulence models applied to CFD drag simulations of a small hatchback vehicle*. No. 2016-36-0201. SAE Technical Paper, 2016. https://doi.org/10.4271/2016-36-0201
[9] Ahmad, Nor Elyana, Essam Abo-Serie, and Adrian Gaylard. "Mesh optimization for ground vehicle aerodynamics." *CFD letters* 2, no. 1 (2010): 54-65.
[10] Yang, Zhigang, and Max Schenkel. *Assessment of closed-wall wind tunnel blockage using CFD*. No. 2004-01-0672. SAE Technical paper, 2004. https://doi.org/10.4271/2004-01-0672
[11] Zingg, D. W., and P. Godin. "A perspective on turbulence models for aerodynamic flows." *International Journal of Computational Fluid Dynamics* 23, no. 4 (2009): 327-335. https://doi.org/10.1080/10618560902776802
[12] Khan, Sher Afghan, Musavir Bashir, Maughal Ahmed Ali Baig, and Fharukh Ahmed Ghasi Mehaboob Ali. "Comparing the effect of different turbulence models on the CFD predictions of NACA0018 airfoil aerodynamics." *CFD Letters* 12, no. 3 (2020): 1-10. https://doi.org/10.37934/cfdl.12.3.110
[13] Daróczy, László, Gábor Janiga, Klaus Petrasch, Michael Webner, and Dominique Thévenin. "Comparative analysis of turbulence models for the aerodynamic simulation of H-Darrieus rotors." *Energy* 90 (2015): 680-690. https://doi.org/10.1016/j.energy.2015.07.102
[14] Karabay, Sami. "Implementation and assessment of k-omega-gamma transition model for turbulent flows." Master's thesis, Middle East Technical University (Turkey), 2022.
[15] Hachimy, Fatima-zahra, Ashraf A. Omar, and Omar Elsayed. "The accuracy of the numerical solution in predicting Ahmed body components drag coefficients." *CFD Letters* 14, no. 5 (2022): 24-32. https://doi.org/10.37934/cfdl.14.5.2432
[16] Versteeg, H. K., and W. Malalasekera. "Computational fluid dynamics." *The Finite Volume Method* (1995): 1-26.
[17] Kuwito, Andre, Steven Darmawan, and Harto Tanujaya. "Aerodynamic analysis of the rear spoiler of hatchback vehicles using SST K-ω turbulence model." In *International Conference on Experimental and Computational Mechanics in Engineering*, p. 159-169. Singapore: Springer Nature Singapore, 2022. https://doi.org/10.1007/978-981-99-7495-5_17
[18] Shankar, G., and G. Devaradjane. "Experimental and computational analysis on aerodynamic behavior of a car model with vortex generators at different yaw angles." *Journal of Applied Fluid Mechanics* 11, no. 1 (2018): 285-295. https://doi.org/10.29252/jafm.11.01.28357
[19] Kamal, Muhammad Nabil Farhan, Izuan Amin Ishak, Nofrizalidris Darlis, Nurshafinaz Mohd Maruai, Rahim Jamian, and R. A. Rashid. "Flow structure characteristics of the simplified compact car exposed to crosswind effects using CFD." *Journal of Advanced Research in Applied Sciences and Engineering Technology* 28, no. 1 (2022): 56-66. https://doi.org/10.37934/araset.28.1.5666
[20] Zhang, Chunhui, Charles Patrick Bounds, Lee Foster, and Mesbah Uddin. "Turbulence modelling effects on the CFD predictions of flow over a detailed full-scale sedan vehicle." *Fluids* 4, no. 3 (2019): 148. https://doi.org/10.3390/fluids4030148
[21] Ekman, Petter, D. Wieser, T. Virdung, and Matts Karlsson. "Assessment of hybrid RANS-LES methods for accurate automotive aerodynamic simulations." *Journal of Wind Engineering and Industrial Aerodynamics* 206 (2020): 104301. https://doi.org/10.1016/j.jweia.2020.104301
[22] Stern, Fred, Robert V. Wilson, Hugh W. Coleman, and Eric G. Paterson. "Comprehensive approach to verification and validation of CFD simulations—part 1: methodology and procedures." *Journal Fluids of Engineering* 123, no. 4 (2001): 793-802. https://doi.org/10.1115/1.1412235.
[23] Muralidhar, K., and T. Sundararajan. *Computational fluid flow and heat transfer*. Narosa Publishing House, 1995.